

Thermal Performance Assessment of an Opaque Ventilated Façade in the Summer Period: Calibration of a Simulation Model through in-field Measurements

Original

Thermal Performance Assessment of an Opaque Ventilated Façade in the Summer Period: Calibration of a Simulation Model through in-field Measurements / Fantucci, Stefano; Marinosci, Cosimo; Serra, Valentina; Carbonaro, Corrado. - In: ENERGY PROCEDIA. - ISSN 1876-6102. - ELETTRONICO. - 111:(2017), pp. 619-628. [10.1016/j.egypro.2017.03.224]

Availability:

This version is available at: 11583/2670413 since: 2017-05-06T23:38:57Z

Publisher:

Elsevier Ltd

Published

DOI:10.1016/j.egypro.2017.03.224

Terms of use:

This article is made available under terms and conditions as specified in the corresponding bibliographic description in the repository

Publisher copyright

(Article begins on next page)



8th International Conference on Sustainability in Energy and Buildings, SEB-16, 11-13 September 2016, Turin, ITALY

Thermal performance assessment of an opaque ventilated façade in the summer period: calibration of a simulation model through in-field measurements

Stefano Fantucci^{a*}, Cosimo Marinosci^b, Valentina Serra^a, Corrado Carbonaro^c

^aDepartment of Energy, TEBE Research Group, Politecnico di Torino, Corso Duca degli Abruzzi 24, Torino 10129, Italy

^bDepartment of industrial engineering (DIN), Alma Mater Studiorum - University of Bologna, viale del Risorgimento 2, Bologna, Italy

^cDepartment of Architecture and Design, Politecnico di Torino, Corso Duca degli Abruzzi 24, Torino 10129, Italy

Abstract

In recent years, several studies have been performed to evaluate the actual contribute of Opaque Ventilated Façades (OVF) as far as the energy efficiency of buildings in the summer period is concerned. In this framework an experimental real-scale module of an OVF was built and tested. Results demonstrated a reduction of ~58% of the thermal load obtained by using a OVF with respect to the unventilated façade configuration. In this paper the experimental measurements were used to calibrate dynamic simulations using ESP-r software, in order to identify the input factors and the key issues mainly impacting on the results discrepancy.

© 2017 The Authors. Published by Elsevier Ltd. This is an open access article under the CC BY-NC-ND license

(<http://creativecommons.org/licenses/by-nc-nd/4.0/>).

Peer-review under responsibility of KES International.

Keywords: Opaque ventilated façade; building simulation; convective heat transfer coefficient; model calibration.

1. Introduction

Opaque Ventilated Façades (OVF) represent an effective solution to prevent the indoor summer overheating with a consequent reduction of the cooling energy demand. In recent years, the adoption of the OVFs has reached high diffusion in both new construction and in the building energy renovation sector. In this context a reliable performance prediction of OVFs via Building Energy Simulation software (BES) assumes growing interest in particular during the design phase of the building envelope.

* Stefano Fantucci. Tel.: +39-011-090-4550.

E-mail address: stefano.fantucci@polito.it

Different approaches are commonly used for the modelling of ventilated façades. Several studies were carried out by means of CFD models (Computational Fluid Dynamic) [1,2] showing a very high reliability, on the other hand most of the studies [3,4,5,6,7] demonstrates that the use of the airflow network (zonal approach) in BES software represent a good compromise between results reliability and low consumption of computational resources in particular when annual simulations are required [8].

In this paper the results of an experimental campaign on a full scale OVF in real operating conditions , carried out in the framework of a Regional funded project (testing different ventilation configurations [9]), have been used to calibrate a computational model, implemented within the Building Energy Simulation program (BES) ESP-r [10] . ESP-r was used since it represents one of the most used software for the simulation of ventilated façades and implement a larger number of convection models compared to other BES programs [11].

2. Methods

The performance of the OVF was assessed through in field experimental measurements in summer period. Furthermore a simulation model was build using the monitored boundary conditions as input data, then the simulation model was calibrated through a step by step procedure aimed at individuate the simulation input which provide the best agreement between predicted and measured temperature results.

An extensive in field experimental monitoring was undertaken in Turin, Italy (Lat. 45.06N, Long. 7,65E), in order to assess the actual energy performance of an OVF in the summer period. Starting from the monitored boundary conditions, used as input data, a simulation model was calibrated through a step by step procedure aimed at identifying the simulation input providing the best agreement between predicted and measured temperature results. Details on the experimental set-up, on the simulation model and on the calibration process are hereafter presented.

2.1. The experimental monitored OVF

The experimental setup of the OVF was built adherent to a laboratory building (LATEC) in Politecnico di Torino (Turin - Italy) as shown in Fig 1a.

The façade has a south-west orientation and the indoor environmental temperature was maintained during daytime at $26\pm 2^{\circ}\text{C}$ while it was in free-floating during night-time. In Fig. 1b the façade configuration is represented and in Table 1, the main thermo-physical properties of each layer constituting the façade are reported.

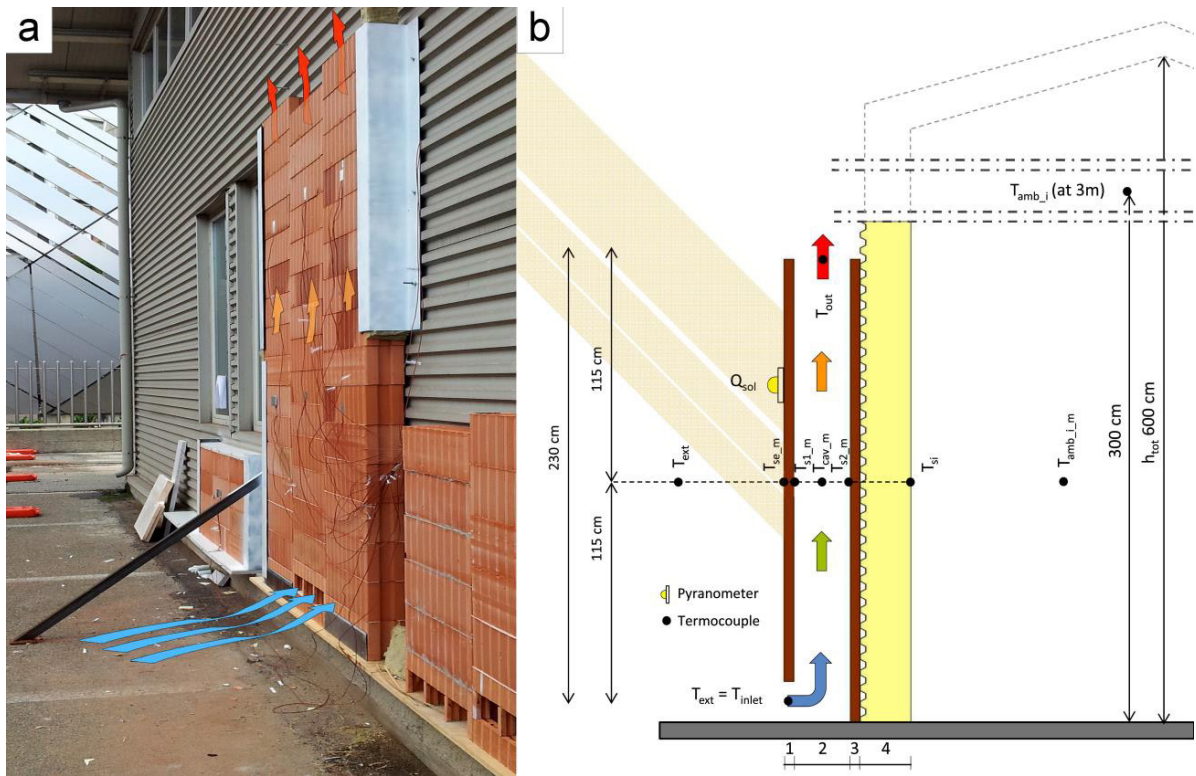


Fig. 1. (a) Picture of the monitored OVF; (b) OVF schematic representation of the sensors position.

Table 1: Wall assembly from outside to inside

n.	name	Thickness (mm)	λ (W/mK)		Specific heat c (J/kgK)	Density ρ (kg/m ³)	Solar absorption coeff. α (-)
			$\lambda_{eq, 10^\circ C}$ (W/mK)	$\lambda_{eq, 50^\circ C}$ (W/mK)			
1	Hollow brick external cladding	35	0.214	0.246	835	1180	0.55
2	Ventilated air cavity	50	-	-	-	-	-
3	Hollow brick internal cladding	35	0.214	0.246	835	1180	-
4	Metal sheet	1		54.00	500	7830	-
5	Mineral wool	100		0.040	840	80-100	-
6	Metal sheet	1		54.00	500	7830	-

The measurements were carried out in summer conditions and 4 reference days (from 11 to 14 September) were selected according to the weather condition, in order to monitor 2 overcast days and 2 sunny days respectively. The evolution of the outdoor and indoor air temperatures and the solar radiation is reported in Fig. 2.

The experimental sensors consist in T-type- thermocouples (nominal accuracy $\pm 0.2K$) for surface and air temperatures and LP02 second class pyranometer (calibration uncertainty $< 1.8\%$) was used for the measurement of the global vertical solar radiation (Fig. 1b).

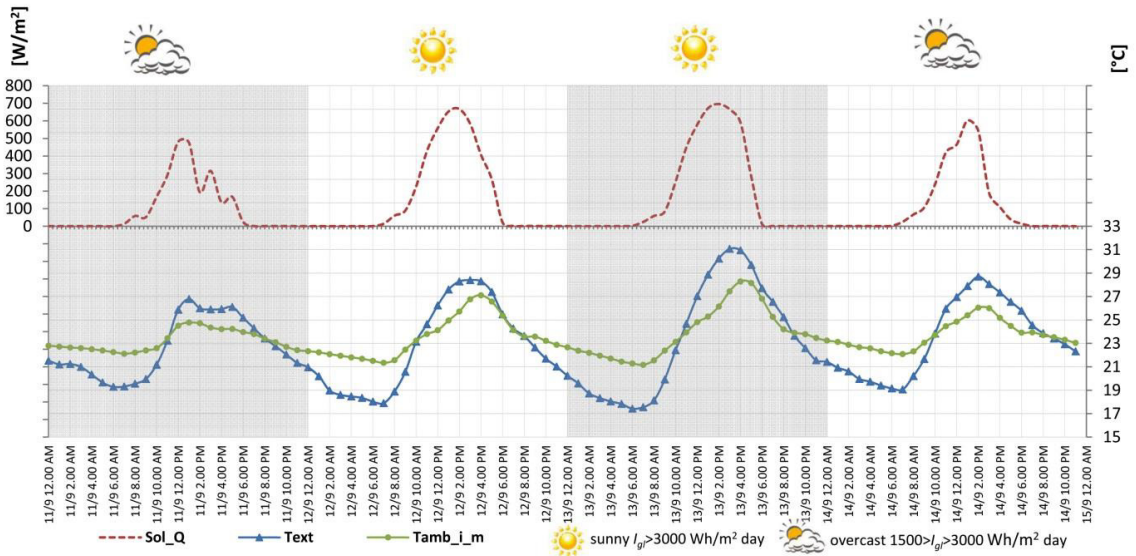


Fig. 2. Environmental condition (air temperature and vertical solar radiation).

2.2. The simulation model

The simulation model is represented in Figure 3a, while the physical properties of each layer used as input data are those reported in table 1.

As described in other research study [5,6,12], to take into account the buoyancy effect, the ventilated air channel was divided in three thermal zones (Figure 3b) and each zone was interconnected to the adjacent one or to the external nodes by air ducts and inlet/outlet air openings (network components). For the simulations, a time step of 5 minutes synchronized with the experimental data-logging was adopted.

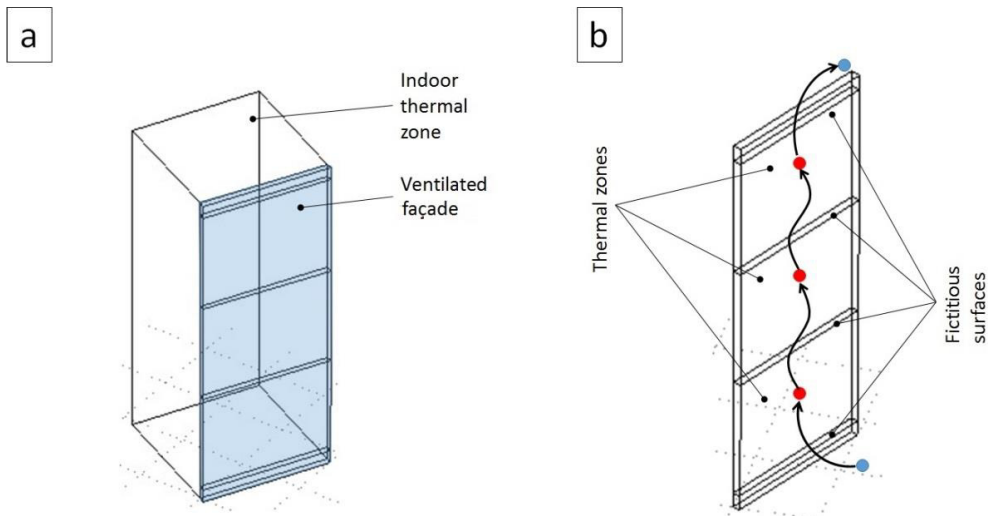


Fig. 3. (a) Simulation model; (b) Façade air network model.

2.3. The model calibration process

Starting from the conventional input data used in BES software (mainly related to: steady state thermos-physical properties, indoor air set point temperature and surface resistances). A step by step simulation process was followed varying the main input parameters in order to match as close as possible the real measured conditions. The calibration process is illustrated in table 2 and the main parameter object of calibration are represented by:

- the thermal conductivity of the external cladding (in STEPS 1,2,3,4 a constant value of thermal conductivity was adopted, while in STEPS 5,6 and 7 a temperature dependent thermal conductivity has been assumed);
- the dry bulk density of the mineral wool insulation layer in the existing wall was considered equal to 100 kg/m^3 in (STEPS 1,2,3,4 and 5), while a value of 80 kg/m^3 was assumed in STEPS 6 and 7;
- the indoor air temperature (in STEPS 1 and 2 a constant value of 24°C was used while the measured hourly temperature profile was assumed in the subsequent simulation steps);
- the convective heat transfer coefficient (different correlations was adopted for the air cavity and for indoor/outdoor surfaces respectively, several correlation was adopted for each surfaces, as shown in table 2);
- the boundary elements of the indoor space (in STEPS 1 and 2 a concrete envelope was set, while in the following steps a fictitious envelope without thermal mass has been assumed);
- the temperature of the indoor surfaces was assumed equal to the indoor air temperature, (in STEPS 1,2 3,4 and 5 the surface temperature was assumed equal to the sensor located in the middle of the façade while in STEPS 6 and 7 the temperature of the sensor located in the middle of the indoor space has been assumed).

Table 2: The step by step calibration process

Simulation STEPS	$\lambda_{\text{ext. cladding}}$	$\rho_{\text{insulation}} [\text{kg/m}^3]$	$T_{\text{air ind}}$	hc air-cavity	hc indoor	hc outdoor	boundary elements	$T_{\text{indoor surfaces}}$
1	$\lambda_{10^\circ\text{C}} (\text{const.})$	100	$24^\circ\text{C} (\text{const.})$	Molina – Maestre [13]	Almandari – Hammond [14]	McAdams [15]	Concrete wall	$T_{\text{s ind}} = T_{\text{amb_i_m}}$
2	$\lambda_{10^\circ\text{C}} (\text{const.})$	100	$24^\circ\text{C} (\text{const.})$	Bar-Cohen – Rosenhow [16]	Almandari – Hammond [14]	McAdams [15]	Concrete wall	$T_{\text{s ind}} = T_{\text{amb_i_m}}$
3	$\lambda_{10^\circ\text{C}} (\text{const.})$	100	Hourly (dyn.)	Bar-Cohen – Rosenhow [16]	Almandari – Hammond [14]	McAdams [15]	fictitious wall	$T_{\text{s ind}} = T_{\text{amb_i_m}}$
4	$\lambda_{10^\circ\text{C}} (\text{const.})$	100	Hourly (dyn.)	Bar-Cohen – Rosenhow [16]	Almandari – Hammond [14]	MoWiTT [17]	fictitious wall	$T_{\text{s ind}} = T_{\text{amb_i_m}}$
5	$\lambda_{\text{(temperature dep.)}}$	100	Hourly (dyn.)	Bar-Cohen – Rosenhow [16]	Almandari – Hammond [14]	MoWiTT [17]	fictitious wall	$T_{\text{s ind}} = T_{\text{amb_i_m}}$
6	$\lambda_{\text{(temperature dep.)}}$	80	Hourly (dyn.)	Bar-Cohen – Rosenhow [16]	Almandari – Hammond [14]	MoWiTT [17]	fictitious wall	$T_{\text{s ind}} = T_{\text{amb_i}}$ (at 3m)
7	$\lambda_{\text{(temperature dep.)}}$	80	Hourly (dyn.)	Bar-Cohen – Rosenhow [16]	Halcrow - low (vert) [18]	MoWiTT [17]	fictitious wall	$T_{\text{s ind}} = T_{\text{amb_i}}$ (at 3m)

Calibration has been done by comparing the measured and predicted surface temperatures. In particular, the temperatures T_{s2} and T_{si} represent the main parameter used for the determination of the efficacy of the ventilated façade to reduce the ongoing heat flow in summer conditions. A good metrics to assess the energy behavior of the OVF is the ΔTL parameter (equation 1), recently introduced in [19]. This performance parameter represent the daily thermal energy reduction obtained by using a ventilated façade (*vent.*) with respect to the unventilated façade configuration (*unvent.*).

$$\Delta TL = 1 - \frac{E_{(vent.)}}{E_{(unvent.)}} = 1 - \left(\frac{C\Delta t \int_{\tau'}^{\tau} [T_{s2}(\tau) - T_{si}(\tau)]_{(vent.)} d\tau}{C\Delta t \int_{\tau}^{\tau'} [T_{s2}(\tau) - T_{si}(\tau)]_{(unvent.)} d\tau} \right) \quad (1)$$

Where: T_{si} is the internal surface temperature, T_{s2} is the temperature of the inside cavity surface (interface 2-3, figure 1a), $E_{(unvent.)}$ is the daily thermal energy load crossing the unventilated façade and $E_{(vent.)}$ represent the daily thermal energy load passing across the ventilated façade. The integer interval in equation 1 is between τ and τ' which indicates respectively the time of day in which the temperature difference between T_{si} and T_{s2} becomes >0 and <0 .

3. Results and discussion

In Figure 4, 5 and 6 the results of the temperature for the 7 simulation STEPS (solid lines) are reported and then compared with the experimental results (dashed red line). For the sake of brevity only the results of the two sunny days was reported. It is possible to observe that the successive simulation STEPS (from STEP 1 to STEP 7) present a better agreement with the measured values as the calibration steps go on.

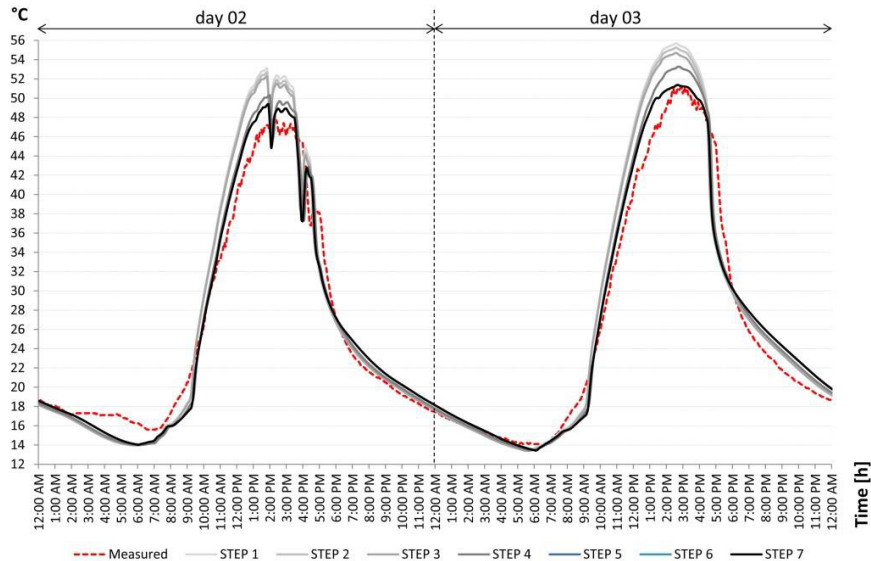
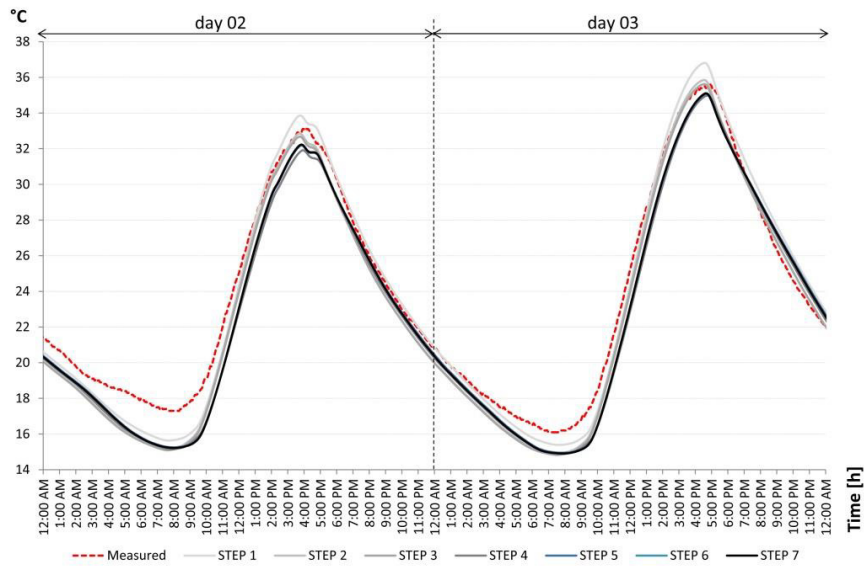
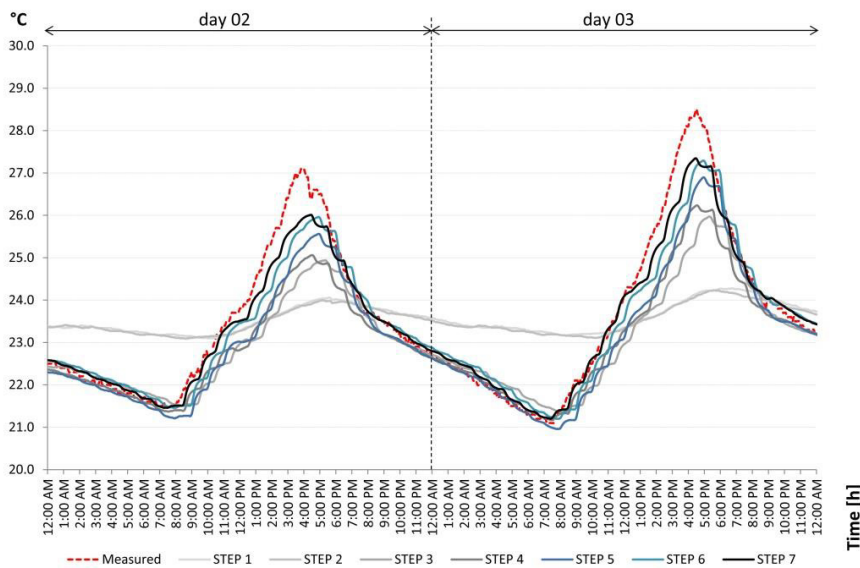


Fig. 4. T_{se} profile.

Fig. 5. T_{s2} profile.Fig. 6. T_{si} profile.

Results show that STEP 7 demonstrate the best agreement with the experimental results except for T_{s2} (Figure 5) in which the maximum divergence are respectively $\sim 1^\circ\text{C}$ for day-time and $\sim 2.5^\circ\text{C}$ for night-time. Nevertheless it is worthy highlighting that for the final calibration process it has been given more importance to the matching of the day-time temperature (used for the calculation of the summer performance of ventilated façade) instead of the night-time.

STEP 5, 6 and 7 are practically overlapped in Fig.4 and 5, while their difference are more evident in Fig.6. This is because these steps differ mainly for the indoor convection coefficient and for the temperature assigned to the indoor boundaries, which have more effect on the calculation of the indoor surface temperature T_{si} .

Furthermore for the analyzed OVF presented in this paper it is possible to identify some general tips useful for a better prediction of the façade performance:

- The use of MoWiTT correlation [17] instead of McAdams correlation [15] allows a better agreement of the external surface temperature;
- Halcrow (low vert.) correlation [18] presents better results for the determination of the indoor surface temperature of the OVF;
- in the absence of precise data about the indoor space it is important to assume a fictitious envelope without thermal mass and set a temperature of the indoor boundary elements equal to the air temperature in the middle of the thermal zone;
- the use of temperature dependent thermal conductivity instead of constant values allow a better matching with the measured data.

3.1. The model reliability

It is to highlight that further simulation STEPS (From STEP 1 to STEP 7) presents a better agreement with the measured values according to the advances of calibration process.

In figure 7 and 8, the predicted temperatures of STEP 7 was plotted against the measured temperatures, the results show that a maximum divergence of 4.7°C for T_{se} , 3.7°C for T_{s1} , 2,5°C for T_{s2} and 0,7°C for T_{si} are obtained, considering a confidence interval of 95%.

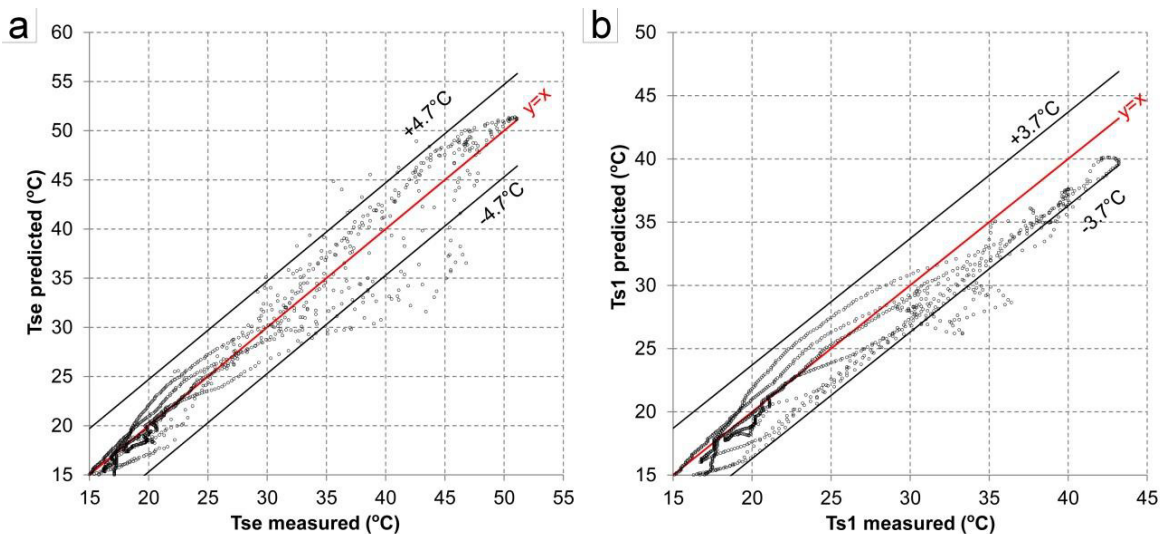


Fig. 7. Correlation between measured and predicted temperatures. (a) T_{se} ; (b) T_{s1} .

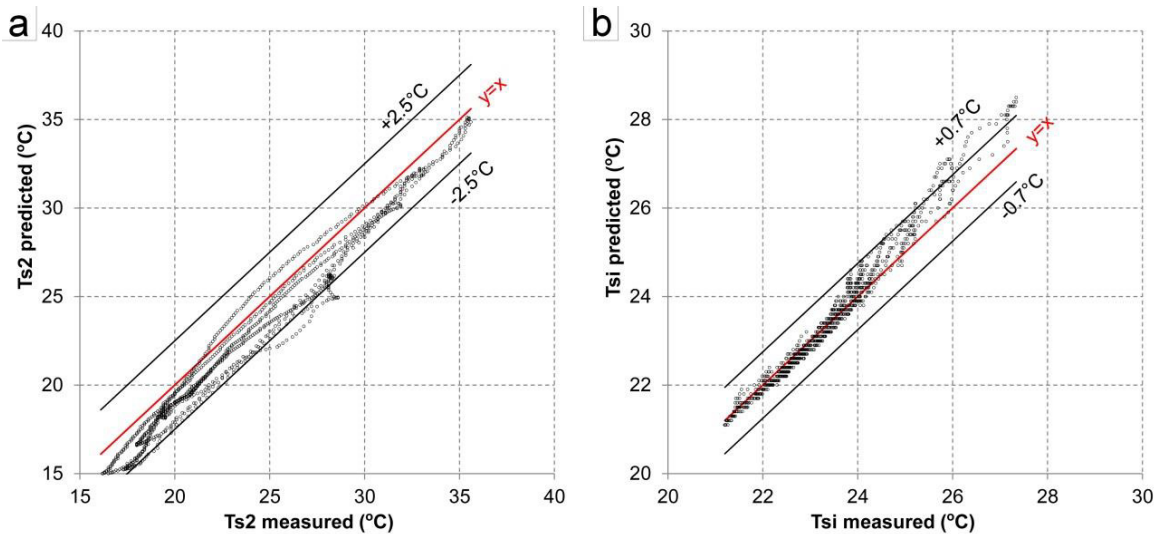


Fig. 8. Correlation between measured and predicted temperatures. (a) T_{s2} ; (b) T_{si} .

In table 3 the results of ΔTL (eq.1) calculated respectively through the predicted and the measured surface temperatures are reported, moreover a reliability rating was attributed depending on the difference between predicted and measured results.

ΔTL presents excellent reliability for the days 02 and 03 characterised by high solar radiation ($I_{sol} > 3500$ [Wh/m² day]); in these two days the difference between predicted and measured values are lower than 4%. On the contrary, the reliability is poor for days 01 and 04, because the calculation of the ΔTL depends by the difference between T_{s2} and T_{si} , which is of relatively low entity in case of overcast/cloudy sky ($I_{sol} < 3000$ [Wh/m² day]).

Nevertheless the reliability of the model remains relatively good considering the whole monitoring period, since in this case the percentage difference between predicted and measured values is around 7%, while the absolute measurement uncertainty is around 8%, due to the fact that the ongoing heat flow assumes more relevance in hot sunny days which are more responsible of the increasing of the cooling energy load compared to overcast/cloudy days.

Table 3: Comparison between the performance parameter of ΔTL calculated respectively through the predicted and the measured temperatures.

days	I_{sol} (Wh/m ² day)	$\Delta TL_{measured}$	$\Delta TL_{predicted}$	$\Delta_{(predict-meas)}$	Reliability rating
01	2382	60% ±11%	82%	21.5%	poor
02	3981	64% ±7%	68%	3.7%	excellent
03	4379	58% ±7%	59%	1.6%	excellent
04	2830	52% ±9%	64%	11.9%	poor
whole period	3730	58% ±8%	66%	7.3%	good

4. Conclusions

The main outcomes of an extensive experimental campaign carried out in the summer period on a OVF, demonstrate its effectiveness in removing the solar loads, with an estimated reduction of the ongoing heat flows, when comparing the ventilated configuration to the unventilated one, ranging between 52% and 64%. In order to provide designers with modeling tools able to reliably predict the energy behavior of this kind of façade a simulation model was built in ESP-r software and a calibration process was performed. Results demonstrate that some input variables such as the surface convection coefficient and the thermal conductivity attributed to the component has an important impact in the correct assessment of the surface temperatures.

As far as the main indicator, i.e. the daily ΔTL , is concerned the study demonstrate that:

- a good reliability of the simulation model is achievable when considering several monitoring days (~7% of difference between predicted and measured results);
- the reliability of the simulation model is influenced by the daily solar irradiance I_{sol} (the higher I_{sol} the higher the model reliability);
- in general the difference between simulated and predicted ΔTL presents values in the range of the measurement accuracy (between 7 and 11%).

The proposed thus a methodology to provide general guidelines for the modelling of ventilated façade and this calibrated model represent a first step for future investigations and for the simulation based optimization of OVFs.

Acknowledgements

The research was developed in the framework of the POLIGHT project “BLOCK-PLASTER – funded by Regione Piemonte. The project was developed in cooperation with DAD_Politecnico di Torino, VIMARK s.r.l., VINCENZO PILONE s.p.a. and NovaRes s.r.l.

References

- [1] Sanjuan C, Sánchez MN, Heras MR, Blanco E. Experimental analysis of natural convection in open joint ventilated façades with 2D PIV, *Build Environ* 2011;46:2314–2325. doi:10.1016/j.buildenv.2011.05.014.
- [2] Giancola E, Sanjuan C, Blanco E, Heras MR. Experimental assessment and modelling of the performance of an open joint ventilated façade during actual operating conditions in Mediterranean climate, *Energ Buildings* 2012;54:363–375. doi:10.1016/j.enbuild.2012.07.035.
- [3] López FP, Jensen RL, Heiselberg P, Ruiz de Adana Santiago M. Experimental analysis and model validation of an opaque ventilated facade, *Build Environ* 2012;56: 265–275. doi:10.1016/j.buildenv.2012.03.017.
- [4] Aparicio-Fernández C, Vivanco JL, Ferrer-Gisbert P, Royo-Pastor R. Energy performance of a ventilated façade by simulation with experimental validation, *Appl Therm Eng* 2014;66:563–570. doi:10.1016/j.applthermaleng.2014.02.041.
- [5] Marinosci C, Strachan P, Semprini G, Morini GL. Empirical validation and modelling of a naturally ventilated rainscreen façade building, *Energ Buildings* 2011;43:853–863. doi:10.1016/j.enbuild.2010.12.005.
- [6] Seferis P, Strachan P, Dimoudi A, Androutsopoulos A. Investigation of the performance of a ventilated wall, *Energ Buildings* 2011;43:2167–2178. doi:10.1016/j.enbuild.2011.04.023.
- [7] Soto Francés VM, Sarabia Escrivá EJ, Pinazo Ojer JM, Bannier E, Cantavella Soler V, Silva Moreno G. Modeling of ventilated façades for energy building simulation software, *Energ Buildings* 2103;65:419–428. doi:10.1016/j.enbuild.2013.06.015.
- [8] De Gracia A, Castell A, Navarro L, Oró E, Cabeza LF. Numerical modelling of ventilated facades: A review, *Renew Sust Energ Rev* 2013;22:539–549. doi:10.1016/j.rser.2013.02.029.
- [9] Fantucci S, Serra V, Perino M. Dynamic Insulation Systems: Experimental Analysis on a Parietodynamic Wall, *Energy Procedia* 2015;78:549–554. doi:10.1016/j.egypro.2015.11.734.
- [10] <http://www.esru.strath.ac.uk/Programs/ESP-r.htm> (Accessed on 09.03.16).
- [11] Mirsadeghi M, Cóstola D, Blocken B, Hensen JLM, Review of external convective heat transfer coefficient models in building energy simulation programs: Implementation and uncertainty, *Appl Therm Eng* 2013;56:134–151. doi:10.1016/j.applthermaleng.2013.03.003.
- [12] Leal V, Erell E, Maldonado E, Etzion Y. Modelling the SOLVENT ventilated window for whole building simulation, *Build Serv Eng Res T* 2004;25:183-195.
- [13] Molina JL, Maestre IR. Energy Exchanges in the Ventilated cavity of the SOLVENT glazing system: Modelling and experimental validation, Appendix Nr.5, SOLVENT final report: Brussels., 2002.
- [14] Almandari F, Hammond GP. Improved data correlations for buoyancy-driven convection in rooms. *Build Serv Eng Res T* 1982;4:106-112.
- [15] McAdams WH, *Heat Transmission*, McGraw-Hill Kogakusha, Tokyo, Japan, 1954.
- [16] Bar-Cohen A, Rohsenow, WM. Thermally optimum Spacing of Vertical Natural Convection Cooled Parallel Plates. *J Heat Trans-T ASME* 1984;106:116-123.
- [17] Yazdani M, Klems JH. Measurement of the exterior convective film coefficient for windows in low-rise buildings. *ASHRAE Trans* 100(1) 1994.
- [18] Halcrow W. Heat transfer at internal building surfaces – Project report to the Energy Technology support unit, (1987).
- [19] Marinosci C, Semprini G, Morini GL, Experimental analysis of the summer thermal performances of a naturally ventilated rainscreen façade building, *Energ Buildings*. 2014;72: 280–287. doi:10.1016/j.enbuild.2013.12.044.